Journal of Engineering and Sustainable Development
https://jeasd.uomustansiriyah.edu.iq/index.php/jeasd
https://doi.org/10.31272/jeasd.26.6.5

Vol. 26, No. 06, November, 2022
ISSN 2520-0917

TECHNICAL RESEARCH

# DESIGN AND SIMULATION OF A MULTI-RECEIVER WIRELESS POWER TRANSFER SYSTEM BASED ON TRANSMITTER CONTROL METHOD

***Muthana J. Mohammed** **Turki K. Hassan**

Electrical Engineering Department, College of Engineering, Mustansiryah University, Baghdad, Iraq

***Received 4/3/2021*** ***Accepted in revised form 10/7/2021*** ***Published 1/11/2022***

**Abstract:** As is usual in a multiple-receiver wireless power transfer (WPT) system based on s-s geometry, the power of load obtained and system efficiency are very sensitive to changes in the number of receivers. An improved multi-receivers WPT system is introduced that ensures the power given for each load remains stable while other receivers enter or exit the system. This study proposes a multiple-load WPT system operated by a class E amplifier. The equivalent system circuit model is analyzed of major parameters such as receiver power, transmitter power, transmission efficiency**,** and each load power allocation. A control circuit is proposed to obtain high transmission efficiency, power control for the transmitter**,** and arbitrary power distribution ratios of receivers for different loads. The cross-coupling between the receiver coils is prevented by adding compensating capacitors at the receiver side in series. This further increases the power stability obtained by loads. Finally, in order to verify the feasibility of the proposed process, simulation results are presented.

**Keywords**: *multiple receivers; WPT wireless power transfer system; S–S geometry; cross-coupling; Class-E inverter.*

## 1. Introduction

With growing the need for more reliable electrical charging methods, WPT has emerged as a modern power supply method. The WPT technology is not restricted by wires and has high mobility, unlike conventional, wire-based power transmission. This has made it a hot topic of research in the field of power transfer, because of its advantages [1], [2]. The WPT is currently widely used for a one-to-one supply of power. Wireless charging for electric cars [3], [4] and for supplying power to medical equipment [5]–[7] has been applied. Moreover, intelligent electronic device wireless charging is also popular [8] as an application that has grown into an industry itself. Wireless charging criteria have also been formulated. The advancement of intelligent technology will be applied on multi-receiver energy supply scenarios including wireless, intelligent home charge, and wireless charging of electric cars. The use of the WPT technology is expected to be more widespread as technology and other emerging power technologies continue to grow rapidly. In addition, it is anticipated that the technology will simultaneously load multiple elements of

**Corresponding Author*: muthanajassim823@gmail.com

electrical equipment (same as wireless fidelity or Wi-Fi, enabling multiple devices to be connected wirelessly). However, various technical problems remain to be overcome when the WPT is applied to a multi-load system (i.e., multiple electrical devices). Firstly, the rise in number of loads involves additional variables and higher nonlinearities with respect to device modeling [9], [10]. Secondly, various loads will require different power requirements (e.g. cell phones, tablets computers, and desk lamps that use the same smart WPT surface have different power demands. Therefore, the power requirements of each of these various types of loads are difficult to guarantee). Third, the properties of the WPT systems suggest that the spatial locations of the electrical equipment also have a major effect on their power [11]. Finally, for different purposes, during the running of the multi-receiver WPT systems, new loads may often enter the system (and the current loads often leave). This would greatly decrease the reliability and efficiency of the system.

This work seeks to find a way to preserve each load's power stability when the number of loads varies. An effective control method is also proposed to achieve optimum system performance. There are four forms of compensation topologies, namely series-to-series (S-S), series-to-parallel (S-P), parallel-to-parallel (P-P), and parallel-to-series (P-S), in this paper, a model (S-S) is presented because it is easy to understand. Many researchers have studied the issue of load power control and obtained substantial results. For example, Ref. [11] assumes a multi-receiver system in which all receiver coils are considered as relay coils, based on (S–S) geometry of compensation. Thus, multiple receivers at different distances will receive the same power. Through coupled-mode theory, another system based on the topology of S-S compensation was analyzed. In this study, a dynamically controlled impedance matching will allow the tunable distribution of power to a multi-receiver system. In Ref. [12], a frequency tracking approach that uses a multi-transmitter system is suggested. Although this can boost overall performance, the power supplied to each recipient cannot be controlled (and thus, each load's efficiency). In Ref. [13], the power stability was achieved in each receiver using a frequency tracking process to continuously control the system's resonant capacitance. There has also been a method for assigning the working frequency for the WPT device, depende**d** on one relay coil and separate frequencies at each circuit [14]. A configuration method was therefore suggested to ensure equal load capacity of each load. In Ref. [15]**,** the secondary-side inductor-capacitor-capacitor (LCC) circuit operating mechanism is examined and, the characteristic of the transmission efficiency under the load of the rectifier is studied. However**,** the secondary structure LCC raises the loading equipment's volume and weight, and a simple structure is more acceptable on the receiver side. Ref. [16] suggests a new approach for matching impedances and power distribution using impedance-inverters on the receiver's ends. The effect of the cross-coupling of the receiving coil in this paper is, however, overlooked and the method for maximizing the efficiency is not suggested. In ref. [17], [18] the requirements for compensation for the effect of cross-coupling between the receiving coils are analyzed and derived. Ref. [19] suggested an optimized multi-load WPT system. The new system uses the LCC topology at the transmitter side to maintain the stability of the power received by the loads. Also, the value of the compensating capacitors was derived to eliminate the effect of cross-coupling between the receiver coils. Ref. [20] suggested an impedance matching network was used on the transmitter side and receiver side of the system to

ensure an optimal distribution of power between the receivers. Ref. [21] proposes a selective omnidirectional MRC WPT with a multiple-receiver system, which owns both omnidirectional and selective power transfer characteristics.

The goal of this paper is to design a multi-load WPT system that ensures each load is provided with stable power while other loads enter or exit the system and improve the overall system efficiency. To achieve these goals:

1- By using the Class-E inverter as a transmitter, the WPT system can achieve high efficiency owing to the Class-E ZVS inverter condition.
2- A control method is suggested for the transmitter current of the multi-receiver WPT systems. The aim of the transmitter side control system is to regulate the transmitted power with the various load's quantities and distributions so that the power transmitted through the transmitter coil can satisfy the demand for each load with improved overall system efficiency. On the other hand, when the other loads enter or exit the system, the power supplied for each load remains constant.
3- There are suggestions to prevent cross coupling effects among receiving coils in order to increase the power stability obtained by loads. Finally, to validate theoretical precision and the feasibility of the suggested method, circuit-level simulations are performed.

## 2. Class-E Inverter Design

The inverter of class E [22]–[24] is composed of dc-power supply $V_{DC}$, choke inductance $L_C$, MOSFET $S$, which acts as a power switch, shunt capacitor $C_S$, load resistance $R_L$, and a series resonant circuit $L_O$ – $C_O$ with equivalent reactance $L_X$, as illustrated in figure 1. The inverter switch is powered by the $V_G$ driving signal. The difference between the current in the choke inductance $I_{DC}$ and the current in a resonant filter $I_{RL}$ passes through the shunt capacitor during the switching-off interval. The current in the shunt capacitor produces the switch voltage $V_S$. The most important operation function of the Class-E inverter is to fulfill the Class-E ZVS condition at a turn-on moment as shown in the figure. 2. The conditions of Class-E operating under zero voltage switching (ZVS) are expressed as [23]:

$$v_S(2\pi) = 0 \text{ and } \left.\frac{dv_S}{d\omega t}\right|_{\omega t=2\pi} = 0 \quad (1)$$

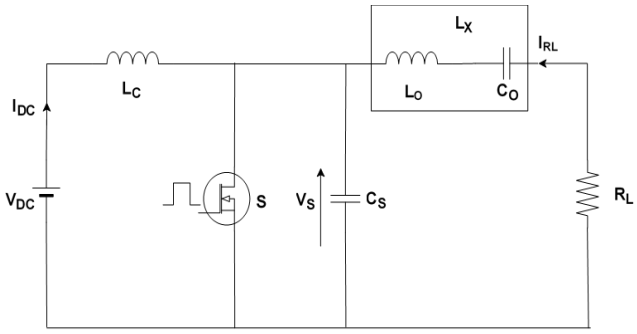


**Figure 1.** Class E inverter circuit topology

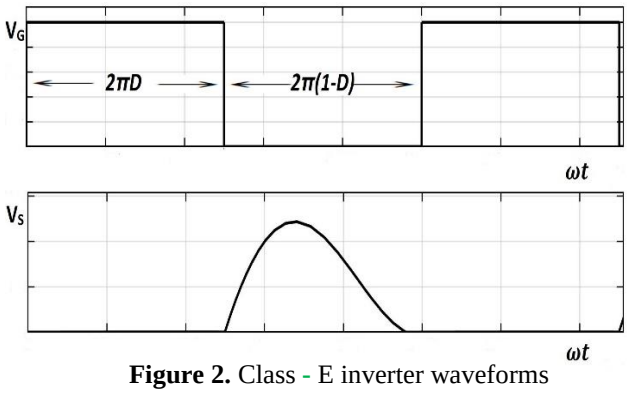


**Figure 2.** Class - E inverter waveforms

The Class-E inverter ensures good power conversion efficiency during high-frequency operations due to Class-E ZVS condition. It is desirable to maintain the duty-ratio $D$ for

MOSFET as 50% when designing the class E inverter for open-loop operations in optimal conditions [24]. However, the component values should be satisfied uniquely for achieving the Class-E ZVS condition. In the ideal case, the power amplifier of Class E is 100% efficient where the load-absorbed active power $P_O$ is equivalent to the DC power supply [22]:

$$I_{DC}V_{DC} = \frac{I_{RL}^2}{2}R_L \quad (2)$$

$$P_o = 0.5768\frac{V_{DC}^2}{R_L} \quad (3)$$

$V_R$ and $V_{LX}$ are the fundamental frequency voltages which can be determined by (Fourier analysis) as [22]:

$$\begin{cases} V_R = -\frac{1}{\pi}\int_0^{2\pi} v_S(\omega t)\sin(\omega t)d\omega t \\ V_{Lx} = -\frac{1}{\pi}\int_0^{2\pi} v_s(\omega t)\cos(\omega t)d\omega t \end{cases} \quad (4)$$

The Class-E power amplifier load network parameter estimation formula can be derived from (4) [22]:

$$\frac{\omega L_x}{R_L} = 1.1525 \quad (5)$$

$$\omega C_S R_L = 0.1836 \quad (6)$$

Where $\omega$ is the angular frequency. On the MOSFET, maximum withstand voltage is [22], [23]:

$$V_{s-max} = 3.562V_{DC} \quad (7)$$

$$L_{C-min} = 3.5\frac{R_L}{f} \quad (8)$$

## 3. Theoretical Analysis

A circuit model for a multiple-receiver WPT system based on the S-S topology that is widely used is shown in Figure 3. $V_{AC}$ is a high frequency voltage source that supplies the system with high frequency alternating current $I_T$. This current produces an electromagnetic field of high frequency in the air as it passes across the transmitter coil, thus building an induced voltage in the different receiving coils so that the system continuously supplies power to the multi-receivers. Transmitter and i$^{th}$ receiving coil inductances are respectively $L_T$ and $L_i$. where (i=1, 2....., n). Moreover, $M_{Ti}$ is the mutual inductance between the transmitter and *i* receiver coil, and $M_{ij}$ is the mutual inductance between receiving coils *i* and *j*. $R_T$ and $R_i$ represent the internal resistors of the transmitter and receiver coils**,** respectively, $C_T$ and $C_i$ are the transmitter and i$^{th}$ receiver compensation capacitances, respectively. The system's operating frequency is $f_o$. In general, the WPT system is using a rectification circuit in the figure. 4, before supplying power to loads to rectify the high-frequency AC**.** Consequently, a constant equivalent resistance $R_{Li}$ can represent each load [19].

$$R_{Li} = R_{\text{Load}} * \frac{8}{\pi^2} \quad (9)$$

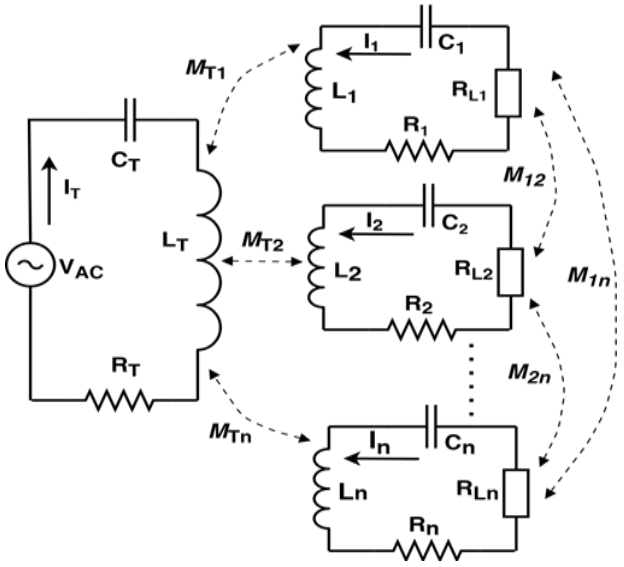


**Figure 3.** A multi-receiver WPT system equivalent circuit based on the S–S geometry

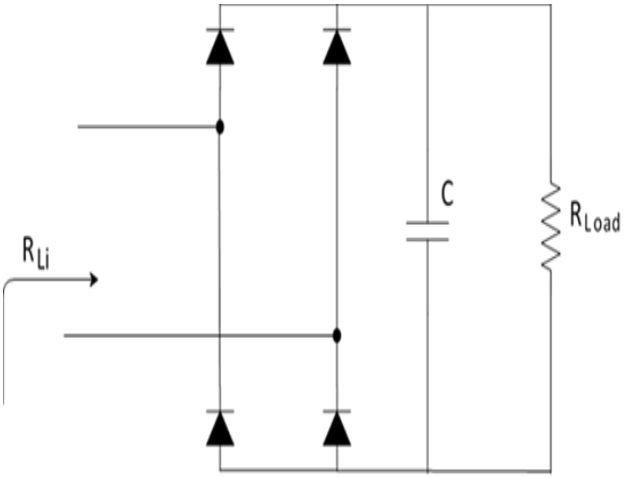


**Figure 4.** The load-equivalent circuit principle

### 3.1. Ideal Model Analysis (Neglecting the Cross Coupling)

The system in Fig. 3 consists of one transmitter and several receiver coils. In order to neglect cross coupling between receiver coils, assume that there are great separations between receiving coils, so that ($M_{ij}$ = 0). Then under resonance condition, $\omega L_T = 1/\omega C_T$ and $\omega L_i = 1/\omega C_i$. The relationships between the high-frequency input voltage supply $V_{AC}$, the current $I_T$ in the transmitter coil**,** and the *Ii* currents of each receiver coil can be described by following the Kirchhoff's Voltage Law [19]:

$$\begin{bmatrix} V_{AC} \\ 0 \\ \vdots \\ 0 \end{bmatrix} = \begin{bmatrix} Z_T & j\omega M_{T1} & \dots & j\omega M_{Tn} \\ j\omega M_{T1} & Z_1 & \dots & 0 \\ \vdots & \vdots & \ddots & \vdots \\ j\omega M_{Tn} & 0 & \dots & Z_n \end{bmatrix} \begin{bmatrix} I_T \\ I_1 \\ \vdots \\ I_n \end{bmatrix} \quad (10)$$

Where, $Z_T = R_T + j\omega L_T + 1/(j\omega C_T)$ and $Z_i = j\omega L_i + 1/(j\omega C_i) + R_i + RL_i$

The transmitter coil is typically larger than the receiving coils in a multi-receiver WPT system to ensure that the system has adequate output capability to meet the power requirements of each load simultaneously. This study assumes that the coil locations of the receivers are specified before designing the system. The reflected impedance by each receiver equivalent to the transmitter coil is [19]:

$$Z_{reflected} = \sum_{i=1}^{n} \frac{\omega^2 M_{Ti}^2}{R_{Li}+R_i} \quad (11)$$

From equation (10) and (11), the transmitter coil current can be obtained as [19]:

$$I_T = \frac{V_{AC}}{Z_{reflected}+Z_T} \quad (12)$$

The principle of mutual inductance shows that after compensation the current for each receiving coil is [19]:

$$I_{i\_uncoupled} = -\frac{j\omega M_{Ti}}{Z_i} I_T \quad (13)$$

Therefore, the power received by each load $P_i$ is [19]:

$$P_i = |\boldsymbol{I}_i|^2 R_{Li} = \frac{\omega^2 M_{Ti}^2 V_{AC}^2}{(R_i+R_{Li})^2 \left(\sum_{i=1}^{n} \frac{\omega^2 M_{Ti}^2}{R_{Li}+R_i}+R_T\right)^2} R_{Li} \quad (14)$$

The system's input power $P_{in}$ is [19]:

$$P_{in} = Real\,(\boldsymbol{V}_{AC}\boldsymbol{I}_T) = \frac{V_{AC}^2}{\sum_{i=1}^{n} \frac{\omega^2 M_{Ti}^2}{R_{Li}+R_i}+R_T} \quad (15)$$

The system loss consists of two major parts, namely the transmitter power loss and the receiver power loss. To easily calculate the entire efficiency of the system, the efficiency of each load $\eta_i$ defined as [19]:

$$\eta_i = \frac{\omega^2 M_{Ti}^2/|Z_i|}{|Z_T|+|Z_{reflected}|} \cdot \frac{R_{Li}}{|Z_i|} \quad (16)$$

The system's total efficiency $\eta$ is [19]:

$$\eta = \sum_{i=1}^{n} \eta_i = \sum_{i=1}^{n} \frac{\omega^2 M_{Ti}^2/|Z_i|}{|Z_T|+|Z_{reflected}|} \cdot \frac{R_{Li}}{|Z_i|} \quad (17)$$

In the above analysis, the major factor affecting the power obtained in each load and system efficiency (when the number of loads changes) is the full reflected impedance $Z_{reflected}$ for all loads in a transmitting part of the system. The

calculation shows that when the system has n+k, n, or n-k loads, the ratio of the current that passing through the $R_{Li}$ load is the following [19]:

$$|I_i(n+k)|:|I_i(n)|:|I_i(n-k)| = \frac{1}{|Z_{ref}(n-k)|+R_t}:\frac{1}{|Z_{ref}(n)|+R_T}:\frac{1}{|Z_{ref}(n+k)|+R_t}$$

### 3.2. Actual Model Analysis (with the Cross Coupling)

Naturally, receiver coils are possibly close together in practice (with their isolation restricted by the power supply range). Therefore, the cross coupling between receiving coils cannot be neglected. Depending on the circuit structure in (Figure 3), the node voltage equation can be re-written as [19]:

$$\begin{bmatrix} V_{AC} \\ 0 \\ \vdots \\ 0 \end{bmatrix} = \begin{bmatrix} Z_T & j\omega M_{T1} & \cdots & j\omega M_{Tn} \\ j\omega M_{T1} & Z_1 & \cdots & j\omega M_{1n} \\ \vdots & \vdots & \ddots & \vdots \\ j\omega M_{Tn} & j\omega M_{1n} & \cdots & Z_n \end{bmatrix} \begin{bmatrix} I_T \\ I_1 \\ \vdots \\ I_n \end{bmatrix} \quad (18)$$

The current that passes through each receiving coil is [19]:

$$\boldsymbol{I_{i\_coupled}} = \frac{-j\omega M_{Ti}\boldsymbol{I_T} - \sum_{j=1, j\neq i}^{n} j\omega M_{ij}\boldsymbol{I_j}}{\boldsymbol{Z_i}} \quad (19)$$

When equation (19) is compared with equation (13), we will find the following:

$$|I_{i-uncoupled}| > |I_{i-coupled}| \quad (20)$$

From Equations (19) and (20), the power received by each load in the real model is smaller compared to the ideal model (for a given set of system parameters and load numbers).

## 4. Coil Design

In this section, simplified equations are given for the appropriate calculation of self-inductance and mutual inductance for the flat-spiral coil used in WPT systems in near-field [26], [27].

### 4.1. Self-Inductance

The self-induction ($L_{self}$) of one circular turn of radius $r$ and wire diameter $d$ is as follows [26]:

$$L_{self}(r,d) = \mu\, r\, \left[\ln\left(\frac{16r}{d}\right) - 2\right] \quad (21)$$

Where μ represents the permeability of the medium around coil. The mutual inductance $M_{ij}$ may be calculated for two perfectly aligned $r_i$ and $r_j$ turns, with a center-to-center distance $D_{ij}$ as [26]:

$$M_{ij} = M(r_i, r_j, D_{ij})$$

$$= \frac{2\mu}{a_{ij}}\sqrt{r_i\, r_j}\left[\left(1 - \frac{a_{ij}^2}{2}\right)k(a_{ij}) - E(a_{ij})\right] \quad (22)$$

$$a_{ij} = 2\sqrt{\frac{r_i\, r_j}{(r_i+r_j)^2 + D_{ij}^2}} \quad (23)$$

Where k($\alpha_{ij}$) and E($\alpha_{ij}$) are the entire first- and second-kinds elliptical integrals, respectively. The self-inductance of a flat, spiral multi-turn coil (Which is widely used in WPT applications) can be calculated as [26]:

$$L_{coil} = \sum_{i=1}^{N_l} L(r_i, D) + \sum_{i=1}^{N_l}\sum_{j=1}^{N_l} M(r_i, r_j, 0)(1 - \varepsilon_{ij}) \quad (24)$$

Where $N_l$ represents the number of turns of the coil, $\varepsilon_{ij} = 1$ for $i = j$ and $\varepsilon_{ij} = 0$ otherwise.

### 4.2. Coupling Coefficient

The magnitude of magnetic flux produced by the transmitter coil which passing through the receiver's coils dictates the necessary coupling coefficient k. Usually, the coupling coefficient is dependent on each coil's geometries, the spacing between coils, and the different orientations of the coils. The value of k can be calculated as [27]:

$$k = \frac{M_{ij}}{\sqrt{L_T L_r}} \quad (25)$$

Where $L_T$ and $L_r$ are the inductance of the transmitter and receiver coils**,** respectively and $M_{ij}$ is the mutual inductance between transmitter and receiver coils. The value of $M$ can be calculated as [27]:

$$M = \sum_{i=1}^{N_T} \sum_{j=1}^{N_R} \mu_0 r_i r_j \int_0^{\pi} \frac{\cos\theta d_\theta}{\sqrt{r_i + r_j - 2 r_i r_j \cos\theta}} \quad (26)$$

Where $N_T$ and $N_R$ are the number of turns of the transmitter and receiver coils respectively, while $\theta$ is the angle between coils planes.

## 5. Optimization of Multi-receiver WPT System Design

### 5.1. Transmitter-side Control

From the above theoretical analysis, the fundamental cause of the change in receiving power by each load, (when a number of loads in a multi-receiver WPT system change) is the difference of the overall reflected impedance $Z_{reflected}$ on the receiver side equivalent to the transmitter side of the system. As a consequence, the current in the transmitter side changes. The design could be improved if the emission current on the transmitter side is set (by a suitably designed controller). The controller provides the received power stability in each load, even if $Z_{reflected}$ was variable. Figure 5, is shown the overall structure of the suggested system. The controller on the transmitter side generates a PWM wave for driving a buck DC-DC converter and, a sinusoidal signal is produced at the end of the transmitter coil with a certain amplitude. In different load conditions, the system suggested in this paper can dynamically modify the transmitter current. Based on Equations (11) and (12), when the number of receivers in the system increase, $Z_{reflected}$ will increase**,** then the transmitter current will decrease. This will lead to a reduction in the received power for each load, and vice versa. The current passing through the transmitting coil is kept at a reference value by changing the width of the PWM wave, while each load obtains enough power to guarantee its optimal operation.

### 5.2. Cross Coupling between Receiving Coils Compensation

The above analysis shows that the implementation of the proposed controller in the transmitter side of the system decreases the propensity for the energy obtained by each load to change due to other loads entering or exiting the system. However, a change in the number of loads would still have an effect on the power stability received by each load, because of the cross coupling between the receiving coils. We suggest resolving this problem by connecting compensatory capacitors in series in the receiving circuits so that the stability of the power received in each load can be further improved. The currents of the receivers in case of cross-connection are similar to those on the ideal model due to the compensation capacitors (for the same load number and system parameters). The value of the compensation capacitance can be calculated by finding the differences between equations (18) and (10) [25]:

$$\begin{bmatrix} 0 \\ 0 \\ \vdots \\ 0 \end{bmatrix} = \begin{bmatrix} 0 & 0 & \cdots & 0 \\ 0 & \mathrm{j}x_1 & \cdots & \mathrm{j}\omega M_{1n} \\ \vdots & \vdots & \ddots & \vdots \\ 0 & \mathrm{j}\omega M_{1n} & \cdots & \mathrm{j}x_n \end{bmatrix} \begin{bmatrix} 0 \\ I_1 \\ \vdots \\ I_n \end{bmatrix} \quad (27)$$

$$X_i = \frac{-\sum_{j=1, j\neq i}^{n} \omega M_{ij} I_j}{I_i} \quad (28)$$

The above analysis shows that given Equation (28) satisfies the compensating capacitive reactance of the series-connected capacitors and it is possible to eliminate the cross-coupling between the receiving coils. This guarantees that

the actual system operates as the ideal system (at which cross-coupling between receiving coils is neglected). Moreover, the impact on the reliability of the power received by each load is greatly reduced as loads join or exit the system. That also makes it possible to convert and then optimize the model for the actual system to a model for an ideal system.

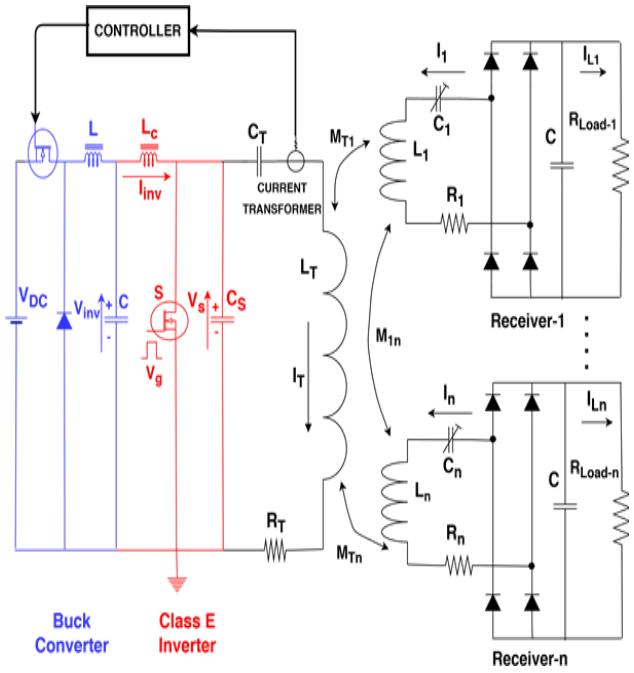


**Figure 5.** A multi-receiver WPT system with a transmitter-side controller

## 6. Simulation Results

The previous analysis shows that a WPT system based on the S-S topology with transmitter control (closed-loop system) proposed in this study should be more optimal than the traditional multi-receiver WPT systems based on S–S geometry (open-loop systems), to supply power for multiple loads. To show that the above theoretical analysis is correct and to make comparison between open-loop and closed-loop systems, MATLAB Simulink was used to simulate the WPT system which consists of one transmitter and two receivers. The closed-loop Simulink model is shown in fig. 6. In this simulation, the power value received for each load is 60 W, i.e. the current, which flows through the loads, is 5 A. Table I includes details of the system parameters simulated.

**Table 1.** System Parameters

| Parameters | Value |
|---|---|
| Operating frequency $f_o$ | 200KH |
| DC voltage Source $V_{DC}$ | 36V |
| Inductance of transmitting coil $L_T$ | 229.833$\mu$H |
| Inductance of receiving coils $L_i$ | 99.8 $\mu$H |
| Transmitter resonant capacitor $C_T$ | 2.817nF |
| Receiver resonant capacitors $C_i$ | 6.345nF |
| Mutual inductance between transmitter and receiver coil $M_{Ti}$ | 1.85835$\mu$H |
| Transmitter internal resistance $R_T$ | 0.128Ω |
| Receiver internal resistance $R_i$ | 0.1Ω |
| Shunt capacitor | 26.76nF |
| Choke inductor | 450 $\mu$H |
| Load resistance $R_{Load-i}$ | 2.4Ω |

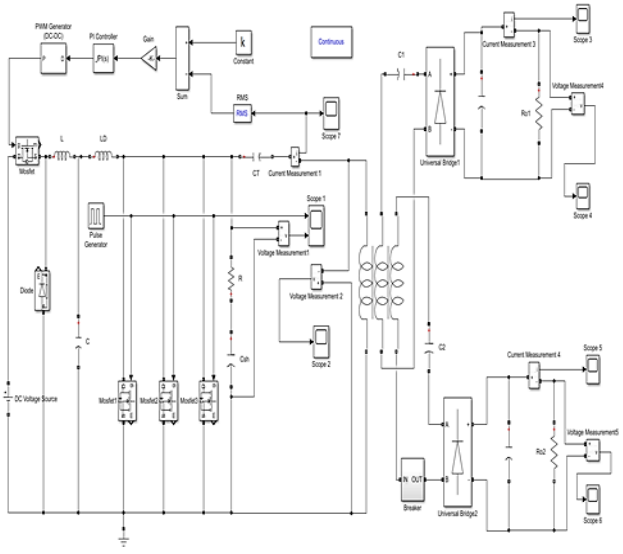

**Figure 6.** The Simulink model for the proposed system

Fig. 7. Shows the simulation waveforms in the case of an open-loop system. It can be seen that the current in the transmitter coil $I_T$ is changed when the number of loads in the system was varied. Therefore, the current and voltage of the load changes, where the power received by the load was 82.36 W with just one load. This level of power is even higher than the original system design power level.

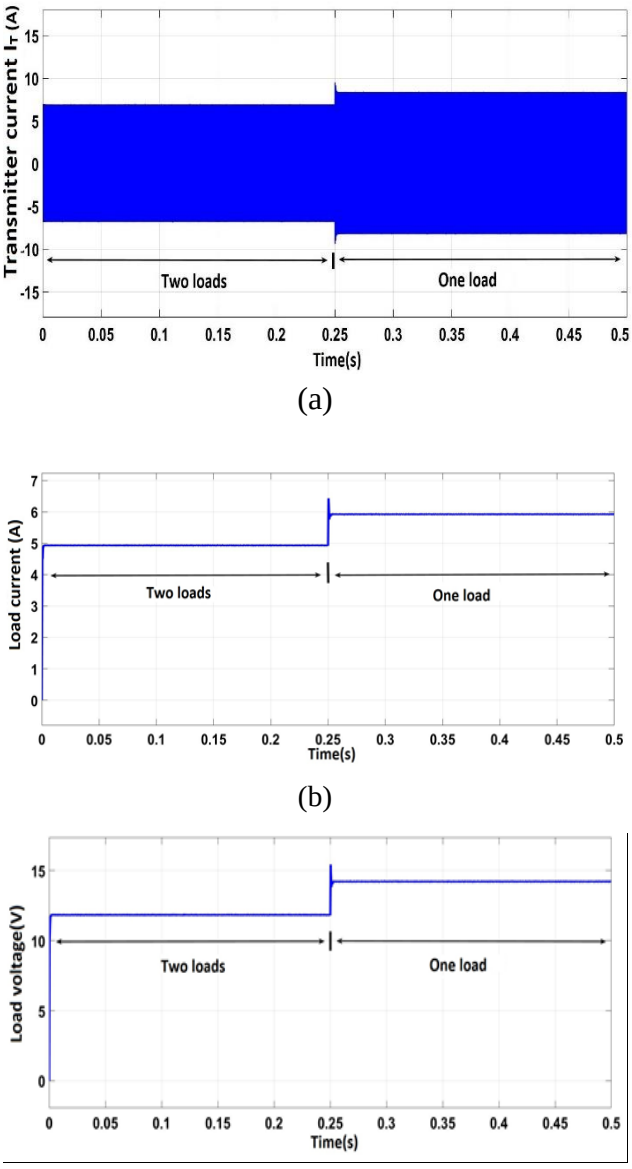


**Figure 7.** Open-loop simulations. (a) Transmitter current (b) Load current (c) Load voltage.

Fig. 8. Shows the simulation waveforms in the case of a closed-loop system (with ignoring cross coupling between receiver coils). It can see that when the number of loads changes from 2 and 1, the transmitting coil current $I_T$ will be essentially unchanged. In addition, the voltage and current variations of the load reached are negligible.

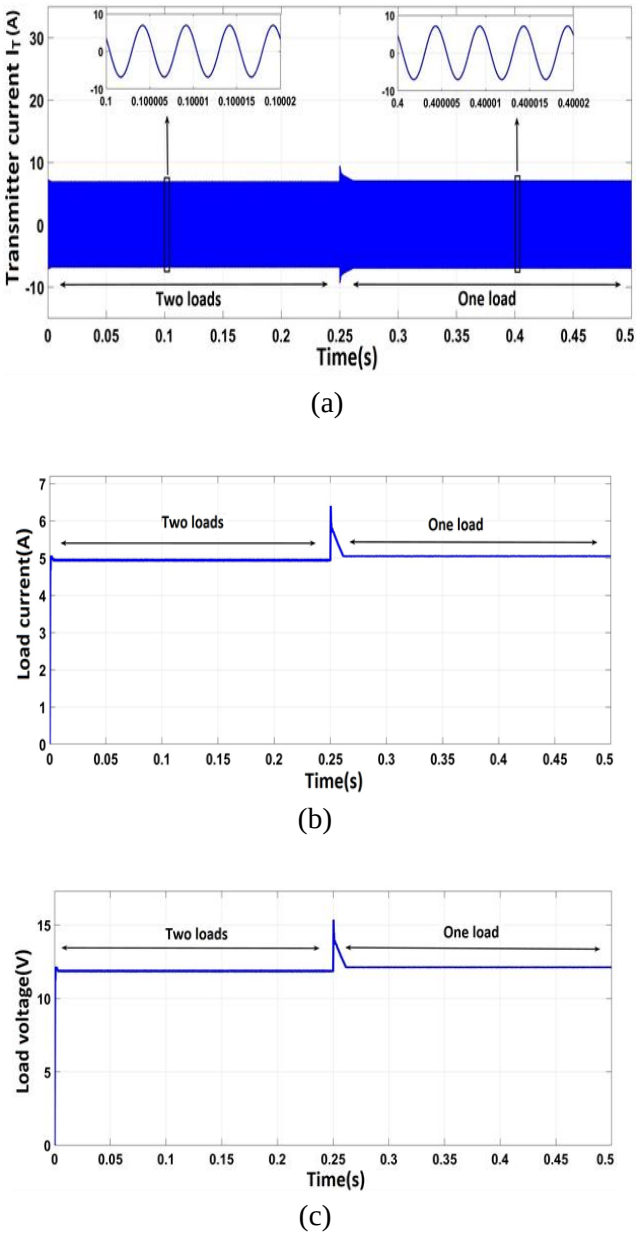


**Figure 8.** Closed-loop simulations. (a) Transmitter current (b) Load current (c) Load voltage.

In this simulation, the power value received in each load is designed to be 60 W, when the current that flows through the load is 5A. Figure. 9 shows that the real power received decreases with rising the number of loads. The cross-coupling between receiving coils is mainly due to this effect. The mutual induction of the receiving coils was found, by calculation, to be $M_{ij}$ = 0.473 μH under the simulation conditions.

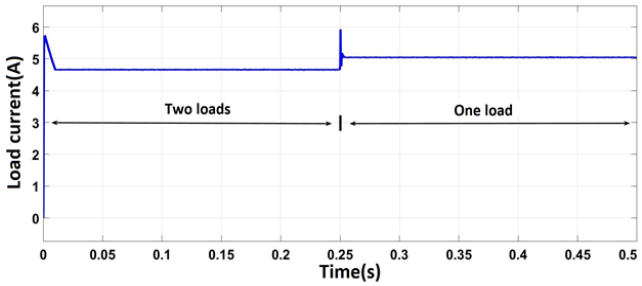


(a)

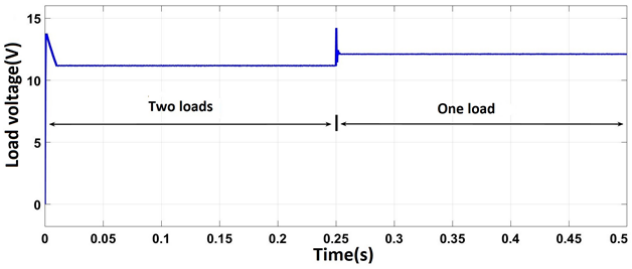


(b)

**Figure 9.** Closed-loop simulations with cross-coupling (a) Load current (b) Load voltage.

Based on equation (28), it is possible to calculate the capacitance of the compensatory capacitors which must be linked in series for each receiver. This would largely remove the effect of a cross coupling between the receiving coils so that the power obtained in each load could stabilize near the designed value. Figure 10 shows the voltage and current of the load when compensation capacitors are used for eliminating the cross coupling between receiving coils.

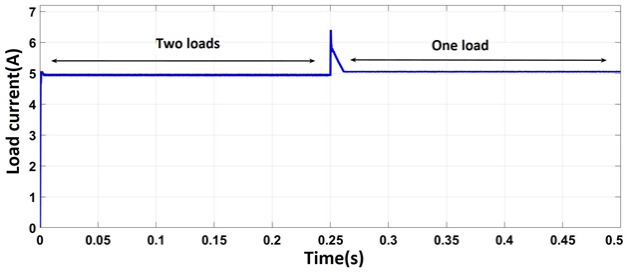


(a)

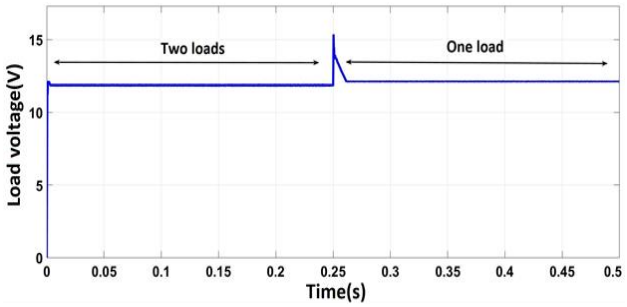


(b)

**Figure 10.** Closed-loop simulations with compensating capacitors (a) Load current (b) Load voltage.

## 7. Conclusions

The aim of this study is to resolve the problem of changes in power obtained in each load in a multiple-receiver WPT system based on the S–S geometry when there is a change in the number of receivers. Therefore, an improved multi-receiver WPT system based on an S-S geometry with a controller on the transmitter side has been proposed. A proposed system ensures that each load's power remains stable. With the implementation of the controller on the transmitter side of the WPT system, the current passing through the transmission coil can be flexibly adjusted and remain unchanged. In order to eliminate the effect of cross coupling between receiving coils, compensation capacitors were connected in series in the receiver circuits. This not only increases the reliability of power obtained in each load but also provides some equivalence between actual and theoretical models. Our results show that the system works

efficiently and is in optimal working condition while meeting the power requirements of each load.

**Acknowledgments**

This work is supported by the Electrical Department/ College of Engineering/ Mustansiriyah University.

**Conflict of interest**

The authors who listed their names in this paper certify that they have no affiliations with or involvement in any organization or entity with any financial interest in the subject matter or materials discussed in this manuscript.

**8. References**

[1] L. Tan *et al.*, "Coordinated source control for output power stabilization and efficiency optimization in WPT systems," *IEEE Trans. Power Electron.*, vol. 33, no. 4, pp. 3613–3621, 2017.

[2] A. Pacini, A. Costanzo, S. Aldhaher, and P. D. Mitcheson, "Load-and position-independent moving MHz WPT system based on GaN-distributed current sources," *IEEE Trans. Microw. Theory Tech.*, vol. 65, no. 12, pp. 5367–5376, 2017.

[3] T. Kan, T.-D. Nguyen, J. C. White, R. K. Malhan, and C. C. Mi, "A new integration method for an electric vehicle wireless charging system using LCC compensation topology: Analysis and design," *IEEE Trans. Power Electron.*, vol. 32, no. 2, pp. 1638–1650, 2016.

[4] A. A. S. Mohamed, A. Berzoy, and O. A. Mohammed, "Experimental validation of comprehensive steady-state analytical model of bidirectional WPT system in EVs applications," *IEEE Trans. Veh. Technol.*, vol. 66, no. 7, pp. 5584–5594, 2016.

[5] X. Li, X. Meng, C.-Y. Tsui, and W.-H. Ki, "Reconfigurable resonant regulating rectifier with primary equalization for extended coupling-and loading-range in bio-implant wireless power transfer," *IEEE Trans. Biomed. Circuits Syst.*, vol. 9, no. 6, pp. 875–884, 2015.

[6] J.-D. Kim, C. Sun, and I.-S. Suh, "A proposal on wireless power transfer for medical implantable applications based on reviews," in *2014 IEEE Wireless Power Transfer Conference*, 2014, pp. 166–169.

[7] S. Bilicz, S. Gyimothy, J. Pavo, L. L. Toth, Z. Badics, and B. Bálint, "Modeling of resonant wireless power transfer with integral formulations in heterogeneous media," *IEEE Trans. Magn.*, vol. 52, no. 3, pp. 1–4, 2015.

[8] A. Berger, M. Agostinelli, C. Sandner, S. Vesti, and M. Huemer, "High efficient integrated power receiver for a Qi compliant wireless power transfer system," in *2016 IEEE Wireless Power Transfer Conference (WPTC)*, 2016, pp. 1–4.

[9] M. Fu, H. Yin, and C. Ma, "Megahertz multiple-receiver wireless power transfer systems with power flow management and maximum efficiency point tracking," *IEEE Trans. Microw. Theory Tech.*, vol. 65, no. 11, pp. 4285–4293, 2017.

[10] L. Sun, H. Tang, and S. Zhong, "Load-independent output voltage analysis of multiple-receiver wireless power transfer system," *IEEE Antennas Wirel. Propag. Lett.*, vol. 15, pp. 1238–1241, 2015.

[11] Y. Zhang, T. Lu, Z. Zhao, K. Chen, F. He, and L. Yuan, "Wireless power transfer to multiple loads over various distances using relay resonators," *IEEE Microw. Wirel. Components Lett.*, vol. 25, no. 5, pp. 337–339, 2015.

[12] D. Ahn and S. Hong, "Effect of coupling between multiple transmitters or multiple receivers on wireless power transfer," *IEEE Trans. Ind. Electron.*, vol. 60, no. 7, pp. 2602–2613, 2012.

[13] B. L. Cannon, J. F. Hoburg, D. D. Stancil, and S. C. Goldstein, "Magnetic resonant coupling as a potential means for wireless power transfer to multiple small receivers," *IEEE Trans. power Electron.*, vol. 24, no. 7, pp. 1819–1825, 2009.

[14] W. Wang, X. Huang, J. Guo, H. Liu, C. Yan, and L. Tan, "Power stabilization based on efficiency optimization for WPT systems with single relay by frequency configuration and distribution design of receivers," *IEEE Trans. Power Electron.*, vol. 32, no. 9, pp. 7011–7024, 2016.

[15] C. Liao, J. Li, and S. Li, "Design of LCC impedance matching circuit for wireless power transfer system under rectifier load," *cpss Trans. power Electron. Appl.*, vol. 2, no. 3, pp. 237–245, 2017.

[16] K. E. Koh, T. C. Beh, T. Imura, and Y. Hori, "Multi-receiver and repeater wireless power transfer via magnetic resonance coupling—Impedance matching and power division utilizing impedance inverter," in *2012 15th International Conference on Electrical Machines and Systems (ICEMS)*, 2012, pp. 1–6.

[17] Fu, M., Zhang, T., Zhu, X., Luk, P. C.-K., & Ma, C. (2016). Compensation of Cross Coupling in Multiple-Receiver Wireless Power Transfer Systems. IEEE Transactions on Industrial Informatics, 12(2), 474–482.

[18] Masataka Ishihara, Kazuhiro Umetani, Eiji Hiraki. (2019). Automatic Active Compensation Method of Cross Coupling in Multiple-receiver Resonant Inductive Coupling Wireless Power Transfer Systems, 2019 IEEE Energy Conversion Congress and Exposition (ECCE).

[19] Linlin Tan, et al, (2019). The Design and Optimization of a Wireless Power Transfer System Allowing Random Access for Multiple Loads, Energies, 12, 1017.

[20] Z. H. Guo and S. E. Dong, "Receiver power allocation and transmitter power control analysis for multiple-receiver wireless power transfer systems," *J. Electron. Sci. Technol.*, vol. 17, no. 4, p. 100009, 2019

[21] Z. Dai, Z. Fang, H. Huang, Y. He, and J. Wang, "Selective Omnidirectional Magnetic Resonant Coupling Wireless Power Transfer With Multiple-Receiver System," *IEEE Access*, vol. 6, no. c, pp. 19287–19294, 2018

[22] F. Wen and R. Li, "Parameter Analysis and Optimization of Class-E Power Amplifier Used in Wireless Power Transfer System," *Energies*, vol. 12, no. 17, p. 3240, 2019.

[23] Y. Wang, J. Song, L. Lin, and X. Wu, "Parameters calculation and simulation of magnetic coupling resonance wireless power transfer system," in *2016 Asia-Pacific International Symposium on Electromagnetic Compatibility (APEMC)*, 2016, vol. 1, pp. 587–590.

[24] T. Nagashima, X. Wei, E. Bou, E. Alarcón, and H. Sekiya, "Analytical design for resonant inductive coupling wireless power transfer system with class-E inverter and class-DE rectifier," in *2015 IEEE International Symposium on Circuits and Systems (ISCAS)*, 2015, pp. 686–689.

[25] M. Pattnaik and N. Kumar, "Optimum Mode Operation and Implementation of Class E Resonant Inverter for Wireless Power Transfer Application," in *2018 IEEE Innovative Smart Grid Technologies-Asia (ISGT Asia)*, 2018, pp. 1074–1078.

[26] S. R. Khan, S. K. Pavuluri, and M. P. Y. Desmulliez, "Accurate modeling of coil inductance for near-field wireless power transfer," *IEEE Trans. Microw. Theory Tech.*, vol. 66, no. 9, pp. 4158–4169, 2018.

[27] B. H. Waters, B. J. Mahoney, G. Lee, and J. R. Smith, "Optimal coil size ratios for wireless power transfer applications," in *2014 IEEE international symposium on circuits and systems (ISCAS)*, 2014, pp. 2045–2048.